

Chapter 6

Two wavelength contouring by iterative phase retrieval using volume speckle field

6.1 Introduction

Shape measurement techniques find their applications in a variety of areas such as quality control in manufacturing industries, surface topography, biomedical imaging, robotics, machine vision, etc[331,332]. Due to technological advancement, techniques using contact as well as non-contact approach have been adopted for shape measurement and surface metrology [333,334]. Especially, in the realm of fabrication of optical devices and components, accurate object deformation measurements along with aspheric shape testing pose a tough challenge [335]. There are many optical techniques available for shape measurements such as triangulation [336,337], fringe projection [338] and interferometric methods [339,340], out of which one of the most effective and widely used optical testing methods for quantifying object (3-D) deformations is the holographic interferometry techniques, as it can inspect larger area of the object, unlike a mechanical probe which takes measurement along a particular direction at a time, giving rise to the need of mechanically scanning the object under study [52,249,285,331–333,341–343]. However, these interferometric techniques while working in the visible regime, encounter problems when dealing with largely deformed aspheric structures [343]. These problems arise due to the use of inverse trigonometric functions (that are periodic) for the phase reconstruction process. The cases wherein the optical path lengths are larger than one time the wavelength, the phase values obtained are equivocal [344] and the periodicity associated with the phase reconstruction process causes the continuous phase information to be wrapped in discrete phase shifts having 2π jumps. Thus, after the reconstruction procedure, an ambiguity will arise as the absolute phase is divided into separated regions with phase value in the range $(-\pi, \pi]$. This causes phase images to contain a large number of 2π jumps in the case of objects having large optical path length changes (steep objects). Thus, to get the true phase information, correct phase cycles needs to be added to each pixel, for instance, by using an algorithm that

detects jumps in the phase image and shifts them up or down depending on the surrounding pixels [345], which may lead to measurement of the phase change for steep objects. This process of getting the continuous phase information from the wrapped phase is known as Phase Unwrapping [346–348]. Researchers have developed and proposed various phase unwrapping algorithm to deal with phase ambiguity [349–360]. A large number of algorithms are available for performing phase unwrapping, but most of these algorithms encounter problems in the case of complex shape measurement, where there is a low fringe modulation, irregular surface brightness, fringe discontinuities and under-sampling [361]. Another constraint while measuring steep objects is imposed by the limited pixel pitch of the sensor because to resolve and analyze one phase jump at least two pixels are required according to the Nyquist criteria [351]. Thus, in an ideal case, it would be preferred not to use phase unwrapping algorithms since they may involve few assumptions and have limitations which may result in an error due to which the real value of phase information may not be obtained [362,363]. Moreover, it is also desirable to reduce the irresolvable phase jumps, associated with steep objects to have resolvable phase fringes.

One of the solutions to tackle the phase unwrapping problem as well as to measure the shape of steep objects is to use a source with a larger wavelength to reduce the number of phase cycles, but it is not feasible to have such a source, as the visible regime consists of wavelengths ranging from 400nm to 700nm. This issue can be addressed by employing the contouring approach for shape measurements using various techniques such as holography, speckle interferometry and electric pattern interferometry (ESPI) [361,364].

As interferometry techniques such as digital holography are being widely used for shape measurement and deformation quantification because of the natural superiority of traceability, large dynamic measurement range, numerical focusing, high sensitivity and resolution [253,256,365], various modifications and advancement has been undertaken to use it as a tool for performing contouring. Holographic contouring can broadly be achieved by a two-wavelength method, two

refractive index method, holographic Moire interferometry, by translating illumination source or object and by light in-flight recording method, etc. [366–377]. All these holographic methods, generally, employ a two-beam off-axis geometry that requires beam steering and beam splitting elements which make the setup complicated and prone to mechanical disturbances. Moreover, these two beam off-axis setups may require adjustment of beam intensity ratio for obtaining high contrast fringes. Thus, a technique that employs a single beam, utilizing fewer components and yielding complex amplitude of the object wavefront will be appreciated. One such modality is the iterative phase retrieval technique, which employs a single beam, and makes use of fewer components to obtain the complex amplitude of the wavefront of interest. The technique relies on the measurement of axial and lateral change in intensity of the wavefront interacting with the object. Multiple intensity patterns of the object are recorded at different axial planes for extracting complex amplitude by iterative use of scalar diffraction integral [182,378,379]. Phase retrieval technique for object complex amplitude reconstruction by imaging volume speckle field at multiple planes and have been reported [380–385]. This technique has already been applied to image biological samples [328,385] as well as deformation measurement [383]. One of the many advantages of employing this iterative phase retrieval approach is the liberty of incorporating a temporally low coherent source such as a LED, which was demonstrated to image micro-objects [386].

Considering such advantages of iterative phase retrieval technique, we have put efforts in the direction of employing it to perform contouring for steep objects by incorporating two sources with different wavelengths.

6.2 Theoretical Background

The phase retrieval methods without using non-interferometric techniques can broadly be classified into two categories: Iterative and deterministic [387]. In the deterministic approach, intensities are recorded on two closely spaced planes which are used in a transport of intensity equation (TIE) to directly (with iterations) compute the phase [388]. Whereas the iterative approach, a technique that

originally evolved from the Gerchberg-Saxton algorithm, uses multiple intensity patterns (diffraction pattern) along with a wave propagation equation and is employed iteratively to determine phase information [297,304]. Apart from the iterative and deterministic approach, one more class which can yield phase information is the probabilistic methods [297,304,389]. The present work is based on the iterative phase retrieval technique, which applies the angular spectrum propagation approach of the scalar diffraction theory to obtain a unique solution to the object wavefront.

The most essential factors, on which the successful wavefront reconstruction depends on, in general, are the sufficient lateral as well as axial intensity variation between two successively recorded intensity patterns [390]. Wavefronts associated with smoothly varying 3D objects, may not produce significant change in the intensity in the lateral as well as axial directions, thus it becomes essential to convert the smoothly varying wavefront (low-frequency intensity pattern) into a high spatial frequency intensity pattern, which may be a volume speckle field generated by employing a diffuser. This formation of speckles generates an appreciable change in the intensity patterns recorded at successive planes [382,390]. In the case of rough objects, the volume speckle field can readily be produced, without using a diffuser, when a coherent source interacts (transmission or reflection mode) with it and thus the necessity of diffuser is eliminated.

Several other factors affect the quality of numerical reconstruction in the case of the iterative phase retrieval technique using volume a speckle field. The primary parameter is the choice of the first sampling plane i.e. the distance between the object and the first plane selected to record the intensity pattern. This parameter can be established by taking into account the lateral speckle size ($\Delta_{lat} = \lambda z / D$), which depends upon the wavelength of the source, size of the object (D) (aperture size) and the distance of the sampling plane from the object (z) [336,391,392]. To satisfy the Nyquist criteria, the speckle size is required to be at least twice the camera pixel size [3,53]. The second important factor that determines the quality and convergence of wavefront reconstruction is the distance between successive

sampling planes (Δz). This factor depends on the appreciable change in the intensity of the speckles (a speckle can be visualized as a cigar suspended in space) in the axial direction while maintaining a sufficient degree of correlation between the intensity patterns recorded at two successive axial planes. The axial speckle size is given by $\Delta_{axial} = 8\lambda (z/D)^2$ [4,382] and Δz should not exceed Δ_{axial} . The third factor that plays a crucial role in the accurate reconstruction of the wavefront is the number of intensity samples. Increasing the number of sampling planes increases the quality of reconstruction as it adds more constraints to the phase retrieval process. But the use of a large number of intensity patterns might affect the reconstruction adversely, since at large distances from the object; the digital array may fail to record higher spatial frequencies (it can collect only small-angle scattering at large distances) which may introduce a recurring error in the phase reconstructions. The optimum number of the intensity sample planes and the number of iterations can be computed by simulations and quality of the reconstruction can be quantified by determining the sum-squared error (SSE) given by

$$SSE = \frac{\sum_{k,l} [I_R(k,l) - I_P(k,l)]^2}{\sum_{k,l} [I_R(k,l)]^2} \quad (6.1)$$

where I_R is the recorded/simulated intensity pattern at an axial plane and I_P is the intensity pattern retrieved by propagation at the same axial plane.

Wavefront (complex amplitude) propagation over short distances using the volume speckle field can be achieved more accurately using the angular spectrum approach to scalar diffraction theory rather than by using the Fresnel-Kirchoff integral with Fresnel approximation, which assumes paraxial propagation [182]. The reason for choosing angular spectrum propagation (ASP) integral is that the propagation of the volume speckle field cannot be assumed as paraxial propagation. The reconstruction process starts by computing the complex amplitude at the first

sampling plane (situated at distance z_1 from the object) using the recorded intensity pattern. Since at this point no phase information is available, a guess phase (ϕ_g) is assumed and is combined with the recorded amplitude (square root of the sampled intensity pattern) to construct the complex amplitude of the wavefront at the first recording plane. This wavefront is propagated to the next sampling plane situated at a distance $z_1 + \Delta z$ using the ASP integral. The phase at this plane is calculated from the resulting complex matrix. So the phase information at this sampling plane is available without any assumption. This process is repeated until the last sampling plane (N^{th}) is reached. The phase of the object wave is corrected at each step during the propagation from one plane to the other. Since the complex amplitude of the wavefront is available at any of the sampling planes, it can be propagated to any desired plane. The convergence of the reconstruction process is tested by comparing the intensity obtained by numerical propagation with the sampled intensity using the SSE value. In practical situations, the number of recorded intensities can be reduced by using the algorithm iteratively. This is accomplished by propagating the wavefront from the last sampling plane back to the first sampling plane by repeating the propagation process between the adjacent planes. The iteration process improves the accuracy of the reconstructions because the input phase at the first plane is derived from the numerical propagation process based on physical experimental data rather than an assumed phase [328,384,386].

The two-wavelength contouring can be applied to the iterative phase retrieval technique using a volume speckle field by recording two sets of intensity patterns using two wavelengths λ_1 and λ_2 . Each set of intensity patterns is supplied as an input in the iterative phase retrieval algorithm separately and the complex amplitude at the first sampling plane is reconstructed (for each wavelength). This reconstructed complex amplitude distribution at the first sampling plane is numerically propagated to the object plane to obtain the object complex amplitude distribution, for both the wavelengths λ_1 and λ_2 . The phase information is extracted from the complex amplitude for both the wavelengths. Since the object information

is in the form of volume speckle, the phase distributions obtained by individual wavelengths are random. But by computing the phase difference, the random phases are eliminated, thereby bringing out the shape information of the object. This resulting phase difference is equivalent to using a synthetic wavelength $\lambda_1\lambda_2/(\lambda_1-\lambda_2)$ [335,343]. The phase difference along with the values of the individual wavelengths can be used to determine the 3D shape profile of the object under investigation. The method can, therefore, be used to shape the quantification of objects.

6.3 Experimental Realization

The experimental setup can be categorized into two configurations with slight alteration depending on the nature of the sample under study i.e. a transparent or reflecting object. The schematic of the experimental setup is shown in Fig.6.1. Where Fig.6.1(a) depicts the geometry used for transparent objects while Fig. 6.1(b) illustrates the setup utilized for reflecting objects.

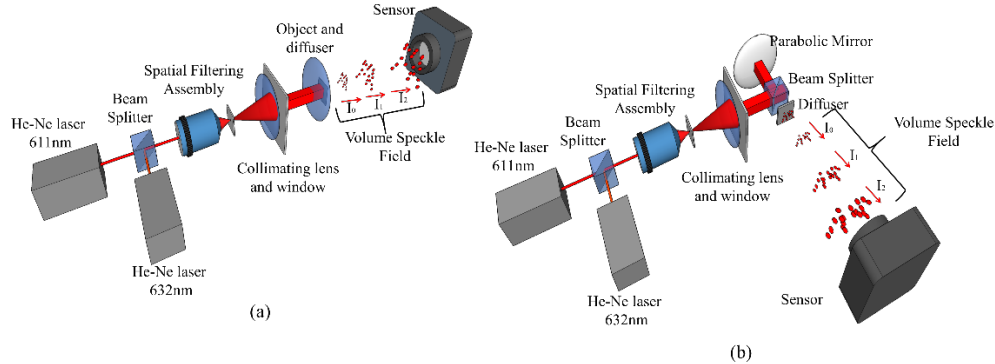


Fig 6. 1: The Schematic of the experimental setup (a) Transmission mode for transparent object (b) Reflection mode for opaque/reflecting objects

As shown in Fig. 6.1 two He-Ne lasers having wavelengths 611nm and 632 nm and the maximum output of 2 mW are employed to obtain a higher synthetic wavelength of $18\mu\text{m}$. A CCD camera (Thorlabs, pixel size $4.65\mu\text{m}\times 4.65\mu\text{m}$, 8-bit dynamic range, 768×1024) is used as a sensor to record the diffraction pattern at different axial planes. Collimated light from each source is made to interact (either in transmission or reflection mode) with the object and the area of illumination is

restricted by a window of 2 mm×2 mm. In the case of transparent objects, the low-frequency diffraction pattern is converted to a high spatial frequency pattern by using a diffuser that generates a partially developed volume speckle beam. This resulting speckle beam is imaged at several axial planes by translating the sensor which is mounted on a linear translation stage. Fig. 6.2 displays the actual arrangement of the experimental setup both for transparent objects (Fig. 6.2(a)) and for reflecting objects (Fig. 6.2 (b)).

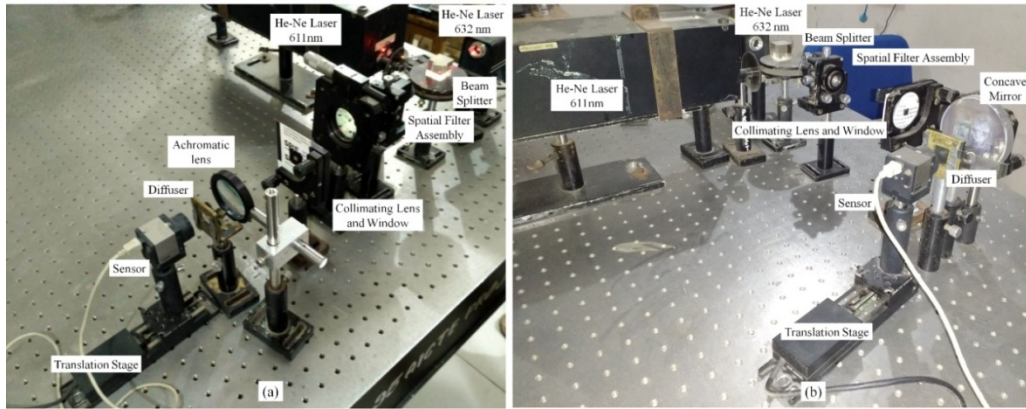


Fig 6. 2: Experimental Setup shape measurement (a) Transmission mode for a positive achromatic lens (b) Reflection mode for a concave mirror

6.4 Simulations

Before proceeding with the experimental realization of the proposed approach, simulations were carried out initially, that employed digital versions of two collimated laser beams (for $\lambda_1=632$ nm and $\lambda_2=611$ nm) which interacted with the digital version of a transparent cone with a circular base of 2mm diameter and optical height (refractive index \times thickness) of 85 μ m as shown in Fig. 6.3.

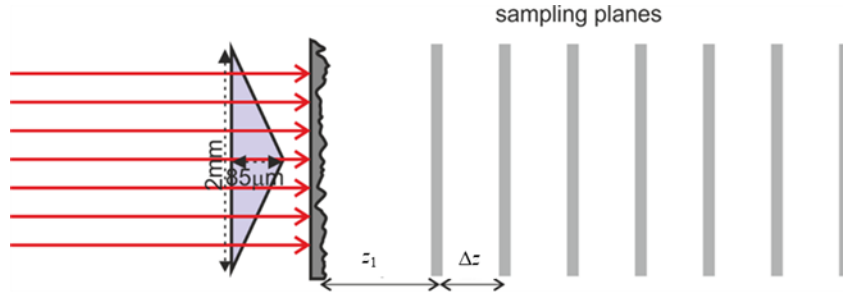


Fig 6. 3: Configuration used for simulation of speckle pattern corresponding to the test object at various axial positions

These beams are then converted into a volume speckle field using a numerical version of a diffuser. The speckle pattern is propagated to different axial planes using angular spectrum propagation integral and the intensity patterns at these planes were simulated as shown in Fig.6.4. The simulated intensity patterns are used iteratively in the phase retrieval algorithm to yield the unique solution for the wavefront at the first sampling plane. The computed complex amplitude distribution is then propagated to the object plane by numerical focusing and the object complex amplitude distribution is extracted. A sensor with a pixel pitch of $4.65 \mu\text{m}$ and 800×800 pixels are considered in the simulations which are the same as the physical sensor that was used in the experimental realization.

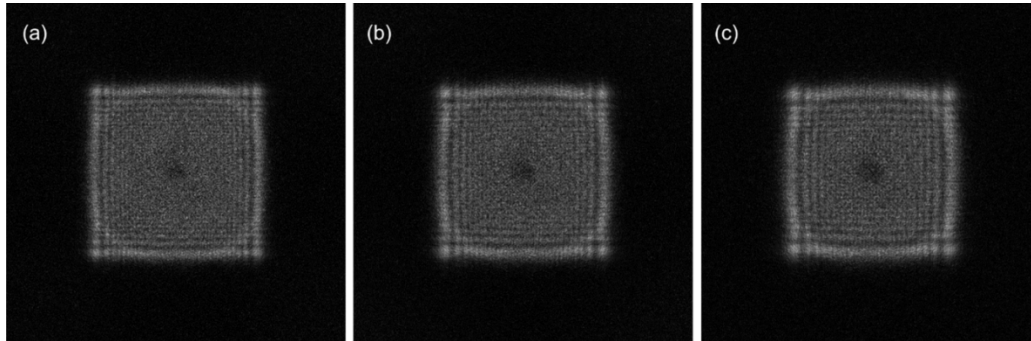


Fig 6. 4: Simulated speckle pattern for the object shown in Fig.6.3 at various distances from the diffuser (a) 30mm (b) 40mm (c) 50mm

It is already been discussed in the previous section that to achieve fast convergence an appreciable change in the intensity along with the lateral as well as axial directions is required. As shown in Fig.6.5 the simulated patterns have sufficient change in intensity along the axial as well as in the lateral direction.

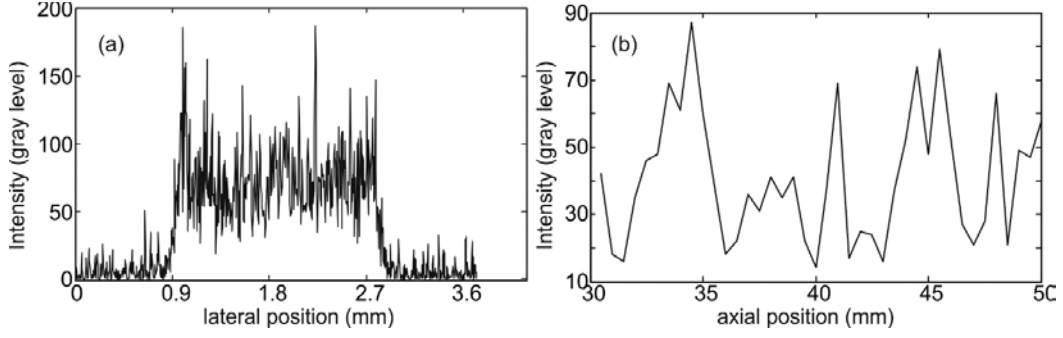


Fig 6. 5: Variation in intensity of the simulated speckle pattern (a) In the lateral direction (b) In the axial direction

Using Eq. (6.1), the sum-squared error (SSE) is employed to determine the convergence of the reconstruction process. Fig. 6.6(a) and Fig. 6.6(b) show the SSE as a function of the number of intensity samples and the number of iterations respectively.

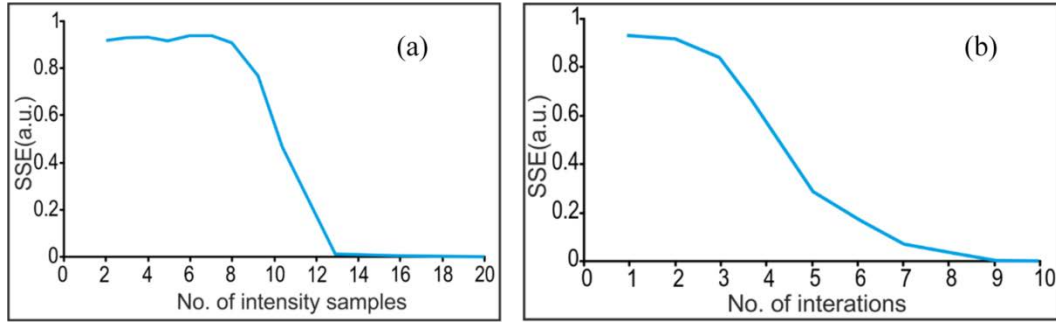


Fig 6. 6: Variation of SSE as a function of (a) Number of intensity samples (b) Number of iterations

Fig. 6.6 suggests that 20 intensity patterns separated by 1 mm axially, along with 10 iterations of the reconstruction algorithm provide accurate and unique solutions of the object wavefront.

To test the applicability of two-wavelength contouring by iterative phase retrieval approach using volume speckle field two sets of intensity patterns are simulated using $\lambda_1=611$ nm and $\lambda_2=632$ nm. Each set contained 20 intensity patterns of the same object separated by 1mm axially. Each set is fed to the phase retrieval algorithm separately and the complex amplitude at the first sampling planes is

reconstructed for both the wavelengths which are numerically focused on the image plane (30mm from the first sampling plane) to generate the object complex amplitude distributions for wavelengths λ_1 and λ_2 . The phase of the object wavefront at the first sampling plane is extracted using the complex amplitude distributions for both the wavelengths (Fig. 6.7(a) and 6.7(b)). Individually, they do not contain any useful phase information, since a ground glass diffuser (which has a random thickness variation) is used to generate the volume speckle field. Therefore, individual wavelengths yield random phase distributions. But computing phase difference eliminates the random phases, which remains the same for the individual wavelengths, bringing out the shape information of the object (Fig. 6.7(c)). This phase difference turns out to be similar to the initial object phase (Fig. 6.7(d)). The phase difference along with the values of the individual wavelengths can be used to determine the 3D shape profile of the object under investigation (Fig. 6.7(e)). The extracted shape is the same as the inputted shape which can be seen from Fig. 6.7(f).

Hence it has been successfully deduced that the method of iterative phase retrieval using volume speckles can, therefore, be used for shape quantification of objects through two-wavelength contouring.

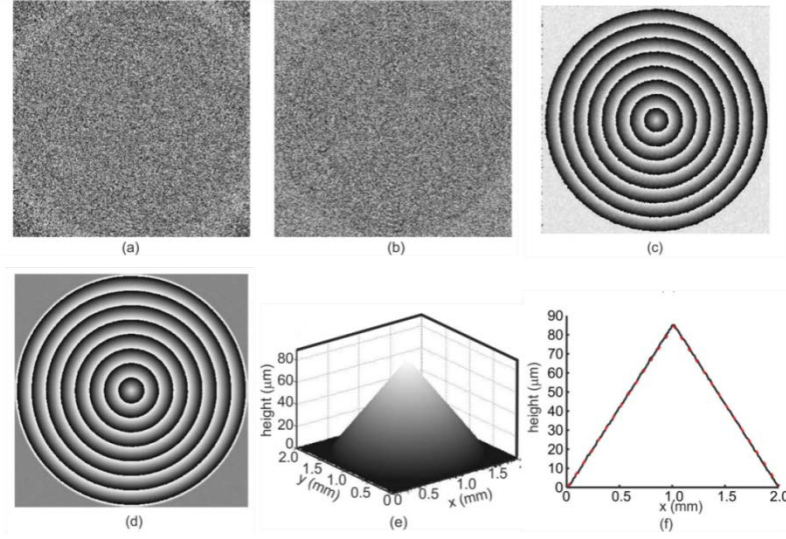


Fig 6. 7: Simulation of two-wavelength contouring. (a) Object phase distribution at $\lambda_1=611\text{nm}$. (b) Object phase distribution at $\lambda_2=632\text{nm}$. (c) Phase difference (contour phase). (d) Inputted contour phase. (e) Shape quantified using synthetic wavelength. (f) Line profile of object shape (red dotted line is obtained from propagation)

6.5 Results

The experiments are conducted in two steps. Initially, a sample that is transparent to the visible radiation is taken under study and then an object with a specularly reflecting surface is studied. A positive achromatic lens is taken as a transparent object while a parabolic mirror is considered as a reflecting surface. The only difference in both the geometry is the way in which the probe beam interacts with the objects under study; in the case of the lens the probe beam is allowed to pass through the lens and gets converted to spherical wavefront which then passes through the ground glass diffuser to generate the volume speckle field whereas in the case of parabolic mirror, the probe is allowed to reflect from its surface by normal illumination using a beam splitter (50:50) where a spherical wavefront is generated upon reflection which later passes through the ground glass diffuser to generate volume speckle field as shown in Fig.6.1 .

Two sets of speckle patterns at 20 axial planes separated by 1mm are recorded for $\lambda_1=611\text{ nm}$ and $\lambda_2=632\text{ nm}$ for both the Transmission and Reflection geometries. These speckles patterns are used in the phase retrieval algorithm to reconstruct the object complex amplitude distribution. The first sampling plane is situated 30 mm

from the diffuser. Fig. 6.8 shows the recorded intensity patterns for $\lambda_1=611\text{nm}$ at several axial planes. The spreading of the laser speckles, as well as an increase in their size, is visible in the Fig. 6.8.

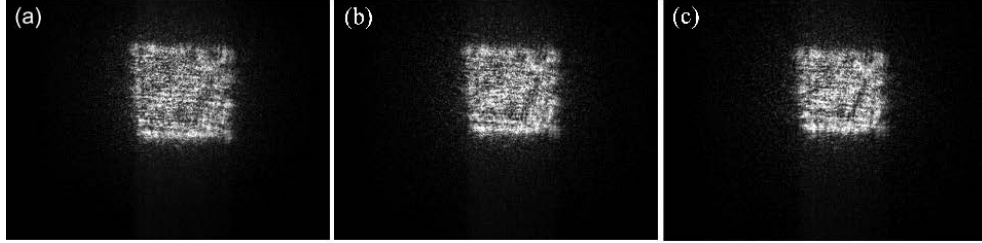


Fig 6. 8: Recorded speckle pattern at different axial positions for $\lambda_1=611\text{nm}$. The positions of the axial planes from the diffuser are (a) 30mm, (b) 39mm, (c) 45mm

A similar set of speckle intensity patterns is recorded for $\lambda_2=632\text{ nm}$. The recorded patterns, in this case, are shown in Fig.6.9.

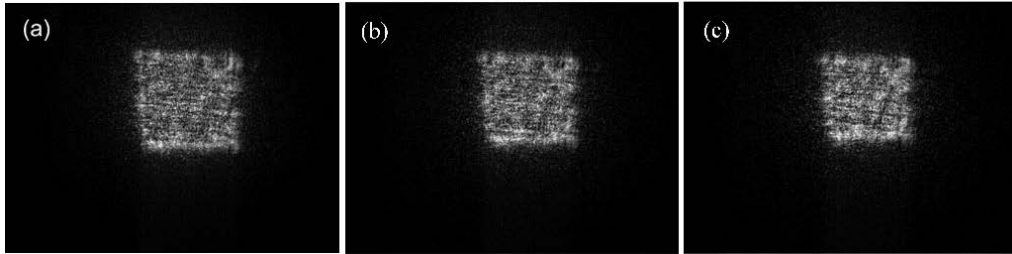


Fig 6. 9: Recorded speckle pattern at different axial positions for $\lambda_2=632\text{nm}$. The positions of the axial planes from the diffuser are (a) 30mm, (b) 39mm, (c) 45mm

These intensity patterns are used in the reconstruction algorithm to compute the complex amplitude of the wavefront at the first sampling plane. This complex amplitude distribution is then propagated to the image plane again using angular spectrum propagation diffraction integral. This leads to the numerical focusing of the wavefront (post-recording processing focusing without the aid of a lens). Fig. 6.10 shows the numerical focusing capability of the technique for $\lambda_1=611\text{ nm}$.

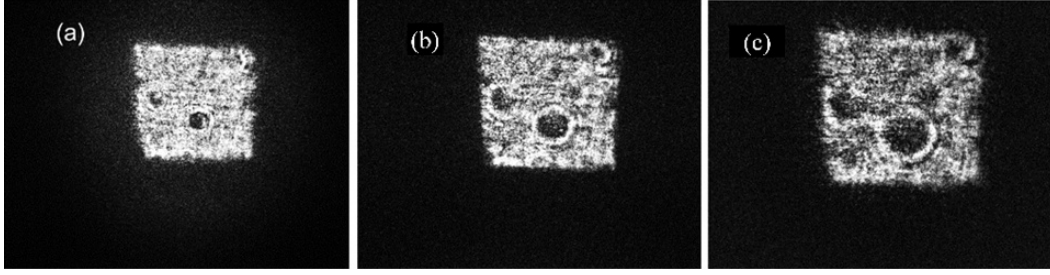


Fig 6. 10: Reconstructed intensity patterns at different axial planes. The distance of the axial planes from the first sampling planes was (a) 5mm, (b) 30mm (best focus) (c) 45mm

Fig. 6.11 shows the reconstructed phase for five axial planes separated by $(\lambda_1/4)$ near the best focus plane. The image series represents the change of focusing distance by one complete wavelength of the source light. It clearly shows the phase reconstruction and very fine focusing capability of the technique.

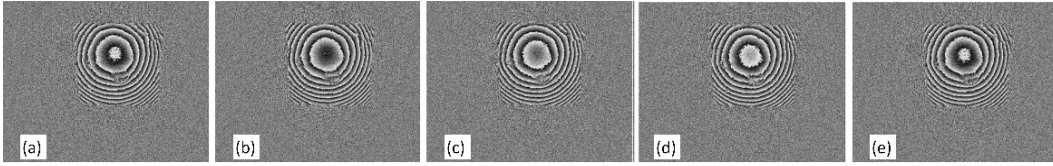


Fig 6. 11: Phase maps obtained for numerical focusing distance over a single wavelength. Each axial plane is separated from the next plane by a distance of $\lambda/4$ ($\lambda=611\text{nm}$). The first plane is situated 30mm from the first sampling plane

It can be seen from the Fig. 6.11 that the center of the phase map does not coincide with the center of the diffuser, indicating that the spherical wavefront was incident an angle on the diffuser. Similar phase maps were obtained using $\lambda_2=632\text{ nm}$. So, ϕ_1 is the phase obtained at the best focus plane for $\lambda_1=611\text{ nm}$ while ϕ_2 is the phase obtained at the best focus plane for $\lambda_2=632\text{ nm}$ as shown in Fig. 6.12.

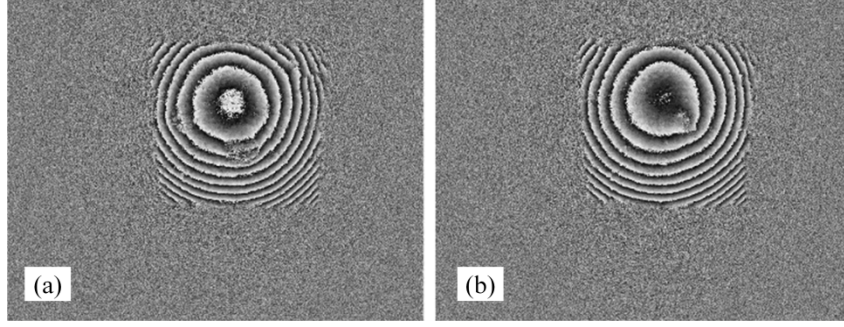


Fig 6. 12: Phase maps at the best focus plane for (a) $\lambda_1=611\text{nm}$ and (b) $\lambda_2=632\text{nm}$

A subtraction of ϕ_1 from ϕ_2 brings out the phase map due to the synthetic wavelength ($\Lambda \sim 18.3 \mu\text{m}$). The phase map due to the synthetic wavelength is shown in Fig. 6.13.

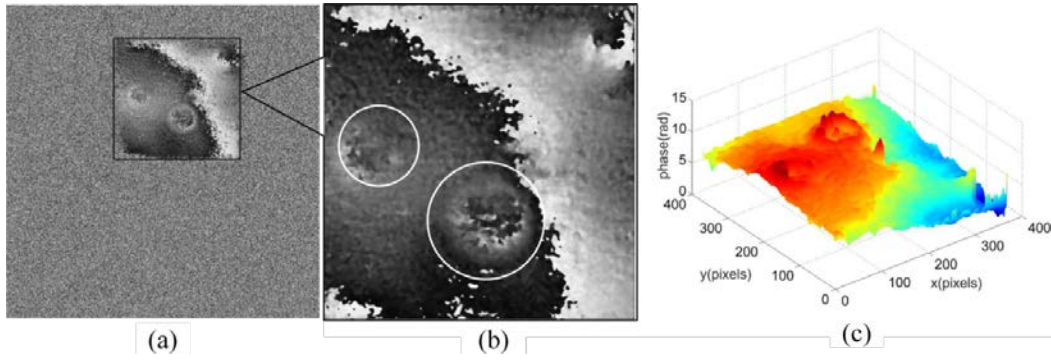


Fig 6. 13: (a) Phase difference ($\phi_1 - \phi_2$) (b) Phase difference inside the area of interest (c) Continuous phase distribution showing the aberrations in the wavefront.

The same procedure is applied in the case of reflection mode where a concave mirror is used as an object. Fig 6.14 shows the contour fringes obtained by computing the phase difference where ϕ_1 is the phase obtained at the best focus plane for $\lambda_1=611 \text{ nm}$ while ϕ_2 is the phase obtained at the best focus plane for $\lambda_2=632 \text{ nm}$ as shown in Fig 6.14

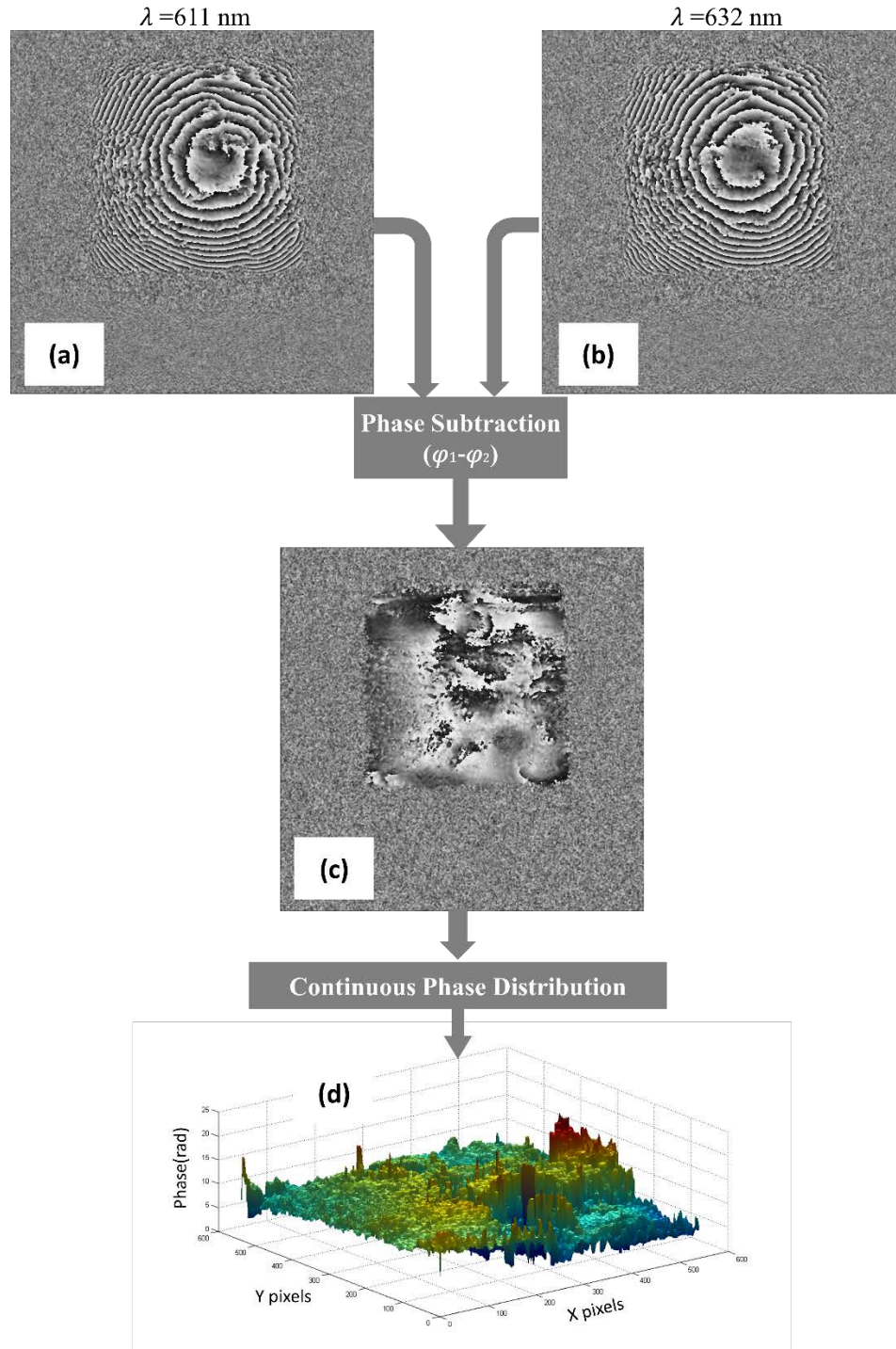


Fig 6. 14: Iterative phase retrieval process for reflection mode (a) Phase maps at the best focus plane for $\lambda_1=611\text{nm}$, (b) Phase maps at the best focus plane for $\lambda_2=632\text{nm}$ (c) Phase difference ($\phi_1 - \phi_2$), (d) continuous phase distribution

6.6 Discussion

Two wavelength contouring is performed utilizing the iterative phase retrieval approach and employing volume speckle field. The use of iterative phase retrieval technique makes the experimental arrangement simple as compared to a conventional two-beam interferometry setup which involves more number of components and careful beam adjustments for desired fringe density and contrast. When the phases obtained for individual wavelengths were subtracted from each other, the contour fringes emerge due to the resulting synthetic wavelength. It can be inferred from the experimental results that the proposed approach can be considered as an alternative method to the existing interferometry methods for shape measurement of steep objects. Moreover, employing two wavelengths helps in avoiding the use of a phase unwrapping algorithm while extracting phase information. The idea of having both the reflection as well as the transmission geometries served the purpose of shape measurement for reflecting as well as transmitting objects.

The experimental results show that two-wavelength contouring can be achieved with the iterative phase retrieval approach employing a volume speckle field by sampling it at multiple axial positions. It is seen that 20 intensity samples separated by 1mm along with 10 iterations of the reconstruction algorithm provide a unique solution of the wavefront at the object plane. The speckle patterns recorded with two wavelengths provide the complex amplitude distribution for these two individual wavelengths at the object plane. When the phases obtained for individual wavelengths were subtracted from each other, the contour fringes due to the resulting synthetic wavelength emerge. The method is ideal for shape measurement of diffusively reflecting objects or transmitting objects. Moreover, with the use of more closely spaced wavelengths, the need for phase unwrapping can also be eliminated.

Chapter 7

Discussion and Future Scope

The work during the course of the thesis was aimed at providing optical solutions to few issues arising in the areas of metrology. Efforts have been made towards designing and developing optical systems which are simple, compact and especially inexpensive. The effectiveness of using laser speckle in various imaging and measurement modalities has been explored. The work in the thesis can broadly be divided into three sections based of the technique with which laser speckles are used and their applications as (1) Laser Speckles with correlations algorithms (2) Laser speckles which lensless Fourier transform digital holography technique (3) Laser speckle with iterative phase retrieval technique.

Laser Speckle correlation algorithm is employed to measure optical and physical quantities by tracking the changes in the speckle pattern. But this technique does not provide phase images and work only on computing the correlation coefficient values. This analysis can be extended by engaging various other statistical algorithms so that correlation can be utilized to obtain useful information. One such approach is to apply Fractal analysis which is considered very crucial while describing natural phenomena. In the case of lensless Fourier transform digital holography, the object information was converted to speckle pattern to facilitate the CCD to collect information from a larger part of the sample. This technique provided the phase data since it involves a reference beam owing to which the principles of digital holography are applied. Iterative phase retrieval approach was explored for performing contouring using two wavelengths. The object beam was converted into speckle field to convert the low spatial frequency into a higher spatial frequency by enhancing the change in recorded intensity pattern between two successive planes. Thus, to summarize the work in the thesis, the laser speckles are employed with various optical techniques to make the measurement and imaging systems simple with better ergonomics and low-cost.

The future plan is to undertake the work on remote sensing of hemodynamics in main blood arteries and in brain by employing a patented approach which is non-

invasive and works on the technique of observing the movement of the secondary speckle patterns generated on the top of the target under investigation when it is illuminated by a spot of laser beam.